schematically shown in Figure 3, a simple reorientation of the copper square-pyramidal moieties might suffice, in principle, to bring about the dimer → uniform-chain transformation without any dramatic change in the geometry of the first coordination sphere around the metal centers or in the occupancy of space. An arrangement of dimers similar to that depicted in Figure 3 exists along the *c* axis of the title compound, and we also note that competition between neighboring copper atoms for bonding to apical chlorine atoms has been shown to be a relevant factor in determining the crystal chemistry of chloride-bridged chain compounds of copper(II).[16–18] In any event, the precise nature of the low-temperature phase of the present compound and the mechanism or reason for the postulated transition are interesting problems that remain open to further studies, particularly low-temperature X-ray studies.

In conclusion, the results presented in this paper confirm the utility of synthesizing new halide-bridged copper(II) compounds with heterocyclic ligands as appropriate candidates for studying the impact of structural phase transitions on the magnetic interactions.[35] As more of these types of systems are prepared and studied, it will hopefully be possible to provide some insight into the mechanisms that underlie the structural changes in them. This problem, of course, is also relevant to the family of distortion models typified by the spin–Peierls instability, i.e., those in which changes in lattice energy and changes in exchange energy are of comparable magnitude.

Registry No. $Cu_2L_2Cl_2{\cdot}2CH_3OH$, 120232-12-4; 8-aminoquinoline, 578-66-5; salicylaldehyde, 90-02-8.

Supplementary Material Available: Tables SI–SIII, listing angles and distances associated with the aromatic rings, thermal parameters, and the derived hydrogen positions (3 pages); a table of calculated and observed structure factors (11 pages). Ordering information is given on any current masthead page.

---

[35] See paper by L. J. de Jongh in ref 2a.

Contribution from the Laboratory for Molecular Structure and Bonding
and Department of Chemistry, Texas A&M University, College Station, Texas 77843

Luminescence and Metal–Metal Interactions in Binuclear Gold(I) Compounds

Christopher King, Ju-Chun Wang, Md. Nazrul I. Khan, and John P. Fackler, Jr.*

Received July 22, 1988

$[Au(dppm)]_2(BF_4)_2$ is phosphorescent in solution (λ_{max} = 593 nm, τ = 21 μs, Φ = 0.31). An SCF–Xα–SW molecular orbital calculation carried out on the model compound $[Au(H_2PCH_2PH_2)]_2^{2+}$ found the Au–Au σ^* HOMO to have 78% Au character. Of this, 41% is from the 6s orbital and 41% is from the $5d_{z^2}$ orbital. The metal–metal interactions are discussed. The 293-nm (ϵ 21 000 M^{-1} cm^{-1}) absorption band is attributed to a $\sigma(p_z) \leftarrow \sigma^*(s,d_{z^2})$ transition. The Au^I_2 emissive state appears to be $^3A_u(\sigma^*)(\sigma)$ (C_{2h} symmetry). The binuclear Au^I_2 compounds $[Au(dppm)]_2Cl_2$, $[Au(CH_2)_2PPh_2]_2$, $[n\text{-}Bu_4N]_2[Au(S_2C{=}C(CN)_2)]_2$, $[Au(CH_2P(S)Ph_2)]_2$, and $[Au(S_2CNEt_2)]_2$ are luminescent in the solid state at room temperature with λ_{max} ranging from 465 to 593 nm and excited-state lifetimes ranging from 1 to 24 μs. $(Ph_3PAu)_2(S_2C{=}C(CN)_2)$ is luminescent at 77 K but not at room temperature. Mononuclear Ph_3PAuCl luminesces in the solid state (λ_{max} = 491 nm, τ = 3 μs).

Introduction

Absorption of light in what has been assigned as a metal-centered p ← d transition leads to phosphorescence from the d^{10} compounds $Pt^0(PPh_3)_3$, $Pd^0(PEt_3)_3$, and $Ni^0(P(O\text{-}o\text{-}tol)_3)_3$.[1,2] Luminescence has also been observed from mononuclear d^{10} Cu^I, Ag^I, and Au^I arylphosphine compounds.[3] For the gold compound the same p ← d transition may be involved, since $Au(PEt_3)_2^+$ and $Au[P(OCH_2)_3CEt]_2^+$,[4,5] which lack aryl groups, and $Au(CH_2PEt_3)_2^+$,[4] containing only Au–C bonds, have absorption bands in the region 200–350 nm assignable to p ← d transitions.

In binuclear compounds the p and d orbitals on the adjacent metal centers mix so that the p ← d transition[4] is replaced by $\sigma(p_z) \leftarrow \sigma^*(d_{z^2})$ (*z* axis through the metal atoms).[1,4,6] Phosphorescence from the binuclear d^{10}–d^{10} compounds $Pt_2(dppm)_3$ and $Pd_2(dppm)_3$ (dppm = $Ph_2PCH_2PPh_2$), in which the metal atoms are three-coordinate, is attributed to this transition,[1] as is phosphorescence from d^8–d^8 complexes, such[6a] as $Pt_2(\mu\text{-}P_2O_5H_2)_4^{4-}$, in which the metals are four-coordinate. The lifetimes of the excited states resulting from these metal-centered transitions sometimes are long enough for bimolecular reactions to occur, such as light-induced oxidative addition of CH_2Cl_2 to $Pd_2(dppm)_3$ to give $Pd_2(\mu\text{-}CH_2)(dppm)_2(Cl)_2$[2] and the reaction of aryl bromide[6b] with $Pt_2(\mu\text{-}P_2O_5H_2)_4^{4-}$.

Emission also has been observed from the heterobimetallic gold(I) compound $AuTl[CH_2P(S)Ph_2]_2$ in solution at room temperature.[7] Neither the Au^I nor Tl^I precursor complexes are luminescent under similar conditions, suggesting that the emission is a result of interactions between the metals. An understanding of the metal–metal interactions and luminescent properties of homobimetallic gold compounds serves as a starting point to develop an understanding of the luminescent properties of heterobimetallic systems containing closed-shell metal ions.

Since $[Au(dppm)]_2^{2+}$ is found to be strongly luminescent in solution, an SCF–Xα–SW molecular orbital study of the model compound $[Au(H_2PCH_2PH_2)]_2^{2+}$ in the chair conformation (C_{2h} point group) was undertaken to determine the nature of the orbitals involved. The suggestion that a bonding interaction between the metals in $[Au(dppm)]_2^{2+}$ may occur by d_{z^2}–s–p_z orbital mixing[8] was investigated. The Au^I–ligand bonding and other details of the Xα calculation, the first to be performed on a binuclear gold compound, are reported in this study. Xα calculations have been performed on the dinuclear d^{10} compounds $[Cu(HNCHNH)]_2$ and $[Ag(HNCHNH)]_2$, which are planar and show metal–ligand π bonding.[9]

---

* To whom correspondence should be addressed.

[1] Harvey, P. D.; Gray, H. B. *J. Am. Chem. Soc.* **1988**, *110*, 2145–2147.

[2] Caspar, J. V. *J. Am. Chem. Soc.* **1985**, *107*, 6718–6719.

[3] Ziolo, R. F.; Lipton, S.; Dori, Z. *J. Chem. Soc., Chem. Commun.* **1970**, 1124–1125.

[4] Ludwig, W.; Meyer, W. *Helv. Chim. Acta* **1982**, *65*(3), 934–943.

[5] Fenske, G. P., Jr.; Mason, W. R. *Inorg. Chem.* **1974**, *13*(7), 1783–1786.

[6] (a) Fordyce, W. A.; Brummer, J. G.; Crosby, G. A. *J. Am. Chem. Soc.* **1981**, *103*, 7061–7064. (b) Roundhill, D. M. *J. Am. Chem. Soc.* **1985**, *107*, 4354–4356.

[7] Wang, S.; Fackler, J. P., Jr.; King, C.; Wang, J. C. *J. Am. Chem. Soc.* **1988**, *110*, 3308–3310.

[8] (a) Dedieu, A.; Hoffmann, R. *J. Am. Chem. Soc.* **1978**, *100*(7), 2074–2079. (b) Mehrotra, P. K.; Hoffmann, R. *Inorg. Chem.* **1978**, *17*(8), 2187–2189. (c) Merz, K. M., Jr.; Hoffmann, R. *Inorg. Chem.* **1988**, *27*, 2120–2126.

0020-1669/89/1328-2145\$01.50/0

Experimental Section

The compounds $[Au(dppm)]_2X_2$ (X = Cl^-,[10] NO_3^-,[11] BF_4^-,[12] and[13] BH_3CN^-), $[Au(CH_2)_2PPh_2]_2$,[14] $[n\text{-}Bu_4N]_2[Au(S_2C{=}C(CN)_2)]_2$,[15] $(Ph_3PAu)_2(S_2C{=}C(CN)_2)$,[16] $[Au(CH_2P(S)Ph_3)]_2$,[17] Ph_3PAuCl,[18] $[Au(S_2CNEt_2)]_2$,[19] and[20] $K_4Pt_2(\mu\text{-}P_2O_5H_2)_4$ were prepared by literature methods and have been structurally characterized. The CH_3CN was distilled from P_2O_5.

Solutions were prepared from crystalline material recrystallized by solvent diffusion from CH_2Cl_2/Et_2O or, for the BH_3CN^- salt, CH_3CN/Et_2O. Emission and excitation spectra, obtained with a Spex Fluorolog 2 fluorimeter, were corrected for instrumental response. Since emission is quenched by oxygen, solutions were degassed with N_2. The exciting radiation for the solids was filtered through a Schott UG1 filter (325–380-nm band-pass) to remove stray light. Exciting wavelengths for solids were chosen to give the strongest signals and hence are not necessarily at absorption maxima. The excitation pulses (ca. 8 ns) for lifetime measurements were from the 355-nm third harmonic of a Quantel YG481 Nd-YAG laser. Emission was monitored with a conventional monochromator–photomultiplier arrangement; digitized signals were passed to a PDP 11/70 computer for analysis. The system has been described fully elsewhere.[21] All measurements were made at room temperature unless otherwise noted.

For the measurement of emission quantum yield, solutions of $[Au(dppm)]_2(BF_4)_2$ in CH_3CN (1.9×10^{-5} M) and $K_4Pt_2(\mu\text{-}P_2O_5H_2)_4$ in pH = 2 aqueous phosphoric acid having equal absorbances at 296 and 368 nm, respectively, were prepared. Their integrated uncorrected emission intensities were compared by using[22] $\Phi = 0.55$ for the emission quantum yield of $K_4Pt_2(\mu\text{-}P_2O_5H_2)_4$. The reference detector within the spectrophotometer was used to correct for differences in intensities of the excitation source at the two excitation wavelengths. Differences in refractive index were ignored. The use of uncorrected emission spectra, necessitated by the lack of correction factors from 750 to 900 nm, probably limited accuracy to $\approx \pm 15\%$.

Attempted Photoreactions. A CH_2Cl_2 solution of $[Au(dppm)]_2(BF_4)_2$ remained luminescent and colorless after irradiation at 300 nm for $^1/_2$ h. A CH_3CN solution of $[Au(dppm)]_2(BH_3CN)_2$ became yellow and stopped luminescing yellow after irradiation at 300 nm for 1 h. Addition of excess $NaBH_3CN$ in THF to $[Au(dppm)]_2(BF_4)_2$ in CH_3CN produced a yellow color within 5 min.

Computational Procedures. Calculations were carried out by the SCF-Xα-SW method.[23] The model compound $[Au(H_2PCH_2PH_2)]_2^{2+}$ was given a chair conformation, with the Au and P atoms lying in the *xz* plane and one C atom lying above and one below this plane. Bond angles and distances, based on those of the structure of $[Au(dppm)]_2(BH_3CN)_2$,[13] were Au···Au = 2.930 Å, Au–P = 2.311 Å, P–C = 1.842 Å, C–H = 1.080 Å, and P–H = 1.440 Å and P–Au–P = 177.3°, P–C–P = 111.1°, and Au–P–C = 111.2°. The compound belongs to the C_{2h} point group with the Au–Au vector along the *z* axis. Starting molecular potentials were constructed from Au(1+) and neutral P and C Herman–Skillman potentials,[24] and from H 1s radial functions. The α values used were those of Schwartz.[25] For intersphere and outer-sphere regions a valence-electron-weighted average of atomic α values was used. The partial wave basis consisted of s-, p-, and d-type spherical harmonics on the Au atoms, s- and p-type on the P and C atoms, and s-type on the H atoms. For the outer-sphere region $l = 5$ was used. Relativistic corrections were applied to the valence levels of Au atoms and the cores of Au, P, and C atoms. Gold 4f orbitals were treated as core orbitals. The SCF calculations were considered to be converged when the shift in potential was less than 0.001 Ryd. The four nonequivalent kinds of hydrogen atoms are combined in Table I. LCAO representations of the converged numerical Xα-SW molecular orbitals were generated by projecting onto a Slater-type atomic orbital basis set[26] that included a double-ζ function for the d orbitals and single-ζ functions for the s and p orbitals of the metal.

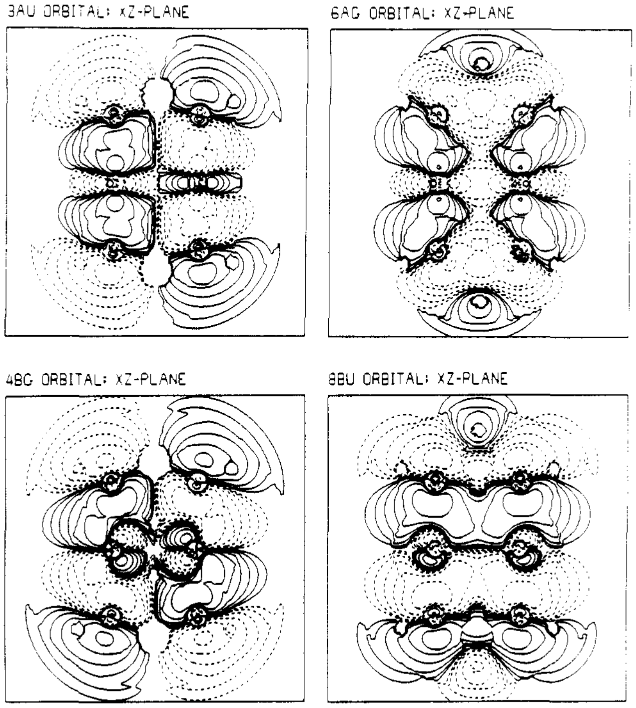

3AU ORBITAL: XZ-PLANE

6AG ORBITAL: XZ-PLANE

4BG ORBITAL: XZ-PLANE

8BU ORBITAL: XZ-PLANE

Figure 1. Contour maps of metal–ligand orbitals. Contour levels are ±0.256, ±0.128, ±0.064, ±0.032, ±0.016, ±0.008, ±0.004, and ±0.002 e $Å^{-3}$.

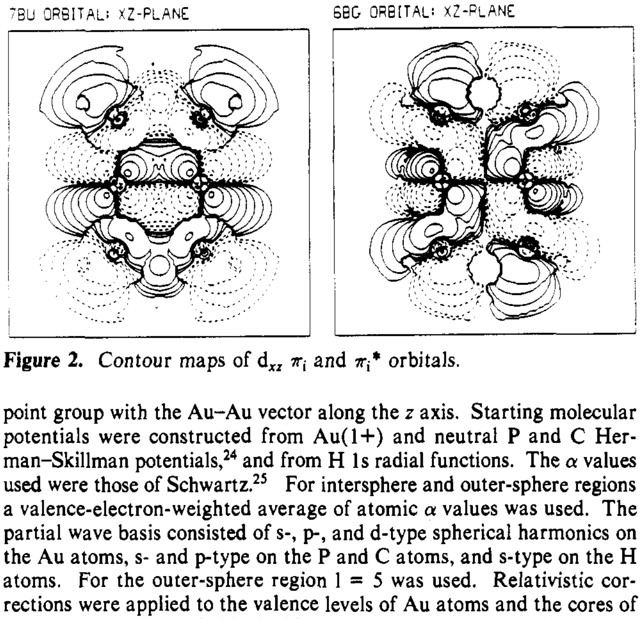

7BU ORBITAL: XZ-PLANE

6BG ORBITAL: XZ-PLANE

Figure 2. Contour maps of d_{xz} π_i and π_i^* orbitals.

Results and Discussion

Xα Calculations. The results of the molecular orbital calculation are shown in Table I. Most of the orbitals can be assigned a single-bonding function. The 16 ligand σ bonds are represented by the $5a_g$, $5b_u$, $3b_g$, and $4a_u$ orbitals and by the 12 lowest energy

---

(9) Cotton, F. A.; Feng, X.; Matusz, M.; Poli, R. *J. Am. Chem. Soc.* **1988**, *110*, 7077–7083.

(10) Schmidbaur, H.; Wohlleben, A.; Schubert, U.; Frank, A.; Huttner, G. *Chem. Ber.* **1977**, *110*, 2751–2757.

(11) Wang, J. C.; Khan, Md. N. I.; Fackler, J. P., Jr. *Acta Crystallogr.*, in press.

(12) Porter, L.; Khan, Md. N. I.; King, C.; Fackler, J. P., Jr. *Acta Crystallogr.*, in press.

(13) Khan, Md. N. I.; King, C.; Heinrich, D. D.; Fackler, J. P., Jr.; Porter, L. C. *Inorg. Chem.*, following paper in this issue.

(14) Basil, J. D.; Murray, H. H.; Fackler, J. P., Jr.; Tocher, J.; Mazany, A. M.; Trzcinska-Bancroft, B.; Knachel, H.; Dudis, D.; Delord, T. J.; Marler, D. O. *J. Am. Chem. Soc.* **1985**, *107*, 6908–6915.

(15) Khan, Md. N. I.; Fackler, J. P., Jr.; King, C.; Wang, J. C.; Wang, S. *Inorg. Chem.* **1988**, *27*, 1672–1673.

(16) Khan, Md. N. I.; Wang, S.; Heinrich, D. D.; Fackler, F. P., Jr. *Acta Crystallogr.* **1988**, *C44*, 822–825.

(17) Mazany, A. M.; Fackler, J. P., Jr. *J. Am. Chem. Soc.* **1984**, *106*, 801–802.

(18) Baenziger, N. C.; Bennett, W. E.; Soboroff, D. M. *Acta Crystallogr.* **1976**, *B32*, 962–963.

(19) Heinrich, D. D.; Wang, J. C.; Fackler, J. P., Jr. *Acta Crystallogr.*, in press.

(20) Alexander, K. A.; Bryan, S. A.; Dickson, M. K.; Heddon, D.; Roundhill, D. M. *Inorg. Synth.* **1986**, *24*, 211.

(21) Foyt, D. C. *Comput. Chem.* **1981**, *5*, 49–54.

(22) Peterson, J. R.; Kalyanasundaram, K. *J. Phys. Chem.* **1985**, *89*, 2486–2492.

(23) (a) Slater, J. C. *Quantum Theory of Molecules and Solids*; McGraw-Hill: New York, 1974; Vol. IV. (b) Johnson, K. H. *Adv. Quantum Chem.* **1973**, *7*, 143. (c) The program was written by M. Cook, Harvard University, and modified locally by B. E. Bursten and G. G. Stanley, Texas A&M University.

(24) Herman, F.; Skillman, S. *Atomic Structure Calculations*; Prentice-Hall: Englewood Cliffs, NJ, 1963.

(25) Schwartz, K. *Phys. Rev. B* **1972**, *5*, 2466; *Theor. Chim. Acta* **1974**, *34*, 225.

(26) Bursten, B. E.; Fenske, R. F. *J. Chem. Phys.* **1977**, *67*, 3138–3145.

Table I. Upper Valence Molecular Orbitals of $[Au(H_2PCH_2PH_2)]_2^{2+}$

			% contribution					Au components[c]			
level	energy, eV	bond[a]	2 Au	4 P	2 C	12 H	I + O[b]				
$10a_g$	−7.436	$\sigma(p_z)$	30	3	1	2	64		94% p_z	2% d_{z^2}	−2% $d_{x^2-y^2}$
$9b_u$	−7.984	$\sigma(p_y)$	13	0	1	2	84		99% p_y	1% d_{yz}	
				HOMO–LUMO Gap							
$7a_u$	−12.606	σ^*	78	5	0	1	16	41% s		41% d_{z^2}	16% $d_{x^2-y^2}$
$6b_g$	−13.629	π_i^*	65	22	8	2	4		−6% p_x	94% d_{xz}	
$8b_u$	−13.721	ML	23	51	12	11	4		−82% p_x	18% d_{xz}	
$9a_g$	−14.147	σ	80	2	1	1	16	−27% s		4% d_{z^2}	68% $d_{x^2-y^2}$
$6a_u$	−14.220	δ^*	88	3	2	4	4			98% d_{xy}	
$5b_g$	−14.236	π_o^*	95	1	0	0	4			100% d_{yz}	
$8a_g$	−14.269	δ	84	3	2	6	4			100% d_{xy}	
$5a_u$	−14.287	σ^*	93	0	0	0	6			50% d_{z^2}	48% $d_{x^2-y^2}$
$4b_g$	−14.310	ML	38	47	0	11	4		22% p_x	73% d_{xz}	
$7b_u$	−14.543	π_i	84	5	3	4	4			100% d_{xz}	
$6b_u$	−14.881	π_o	94	0	0	0	6			100% d_{yz}	
$7a_g$	−15.402	σ	90	1	1	1	7	17% s		79% d_{z^2}	3% $d_{x^2-y^2}$
$4a_u$	−15.719	L	3	49	27	14	6				
$3b_g$	−16.039	L	17	44	23	11	5			98% d_{xz}	
$6a_g$	−16.353	ML	25	30	29	16	1	−2% s	26% d_{xy}	28% d_{z^2}	−44% $d_{x^2-y^2}$
$5b_u$	−16.498	L	3	28	27	40	1				
$5a_g$	−16.852	L	18	16	27	40	0	5% s	15% d_{xy}	15% d_{z^2}	−65% $d_{x^2-y^2}$
$3a_u$	−17.684	ML	50	39	1	10	0	18% s		−18% d_{z^2}	64% $d_{x^2-y^2}$

[a] Major bond component. ML = metal–ligand; π_2 and π_o indicate π bonds in and out of the Au_2P_4 (xz) plane. [b] I + O = orbital density in intersphere and outer-sphere regions. [c] Relative signs of different components on same atom are indicated.

Table II. Emission Properties[a] and Au···Au Separations of Au(I) Compounds

	Au···Au, Å	λ_{max}, nm	τ, μs
$[Au(S_2CNEt_2)]_2$	2.787 (1)	554	1.3
$(n\text{-}Bu_4N)_2[Au(S_2C{=}C(CN)_2)]_2$	2.796 (1)	515	24[b]
$[Au(dppm)]_2(BH_3CN)_2$	2.931 (1)	571	15[b]
$[Au(dppm)]_2Cl_2$	2.962 (1)	467	5.5[b]
$[Au(CH_2)_2PPh_2)]_2$	2.977 (1)	483	
$[Au(CH_2P(S)Ph_2)]_2$	3.040 (1)	465	
$(Ph_3PAu)_2(S_2C{=}C(CN)_2)$	3.156 (1)	500	2.3[b,c]
Ph_3PAuCl	6.990	461, 493	3[b]

[a] At room temperature in the solid state unless stated otherwise. [b] First-order component only. [c] 77 K.

orbitals, which are not included in the table because each has less than 10% metal character.

The orbitals used by gold for metal–ligand σ bonding are best described as combinations of s, p, and d atomic orbitals. The empty 6s orbital mixes with d_{z^2} and $d_{x^2-y^2}$ in both $3a_u$ and $6a_g$; the empty $6p_x$ orbital mixes with d_{xz} in $4b_g$ and $8b_u$ (Figure 1). Mixing of s and p atomic orbitals is symmetry-forbidden here. Such mixing is also forbidden in, e.g., linear $(PPh_3)_2Au^+$ in C_{2h}, D_{3h}, D_{3d}, and $D_{\infty h}$ symmetries, but sp mixing is symmetry-allowed in linear PPh_3AuCl in C_{3v} or any other noncentric symmetry.[27]

If metal–metal interactions are now examined, the $\delta(d_{xy})$ and $\delta^*(d_{xy})$ orbitals $8a_g$ and $6a_u$ are separated by only 0.049 eV, showing that δ interactions are negligible. The d_{yz} π_o and π_o^* orbitals $6b_u$ and $5b_g$ are separated by 0.645 eV, suggesting that dπ interactions are significant. (The subscripts o and i indicate out of and in the Au_2P_4 plane.) The d_{xz} π_i and π_i^* orbitals $7b_u$ and $6b_g$ have some M–L character (Figure 2), which accounts for their greater separation of 0.914 eV. Some π_i^* character is also found in $4b_g$ and $3b_g$.

The four metal–metal σ and σ^* orbitals (Figure 3) have 6s, $5d_{z^2}$, and $5d_{x^2-y^2}$ components. $7a_g$ is simply $\sigma(d_{z^2})$. $9a_g$ has $\delta(d_{x^2-y^2})$ character, but because the 6s orbital is mixed into it, it is considered a σ orbital. In $5a_u$, d_{z^2} and $d_{x^2-y^2}$ combine to give what may be viewed as $\sigma^*(d_{z^2-y^2})$. The two again combine in the HOMO $7a_u$; this orbital resembles $\sigma^*(d_{z^2-x^2})$, but because 6s character replaces some $d_{x^2-y^2}$ character, it is better described as $\sigma^*(s,d_{z^2})$.

The formal metal–metal bond order is zero, as it also is in $[Cu(HNCHNH)]_2$ and $[Ag(HNCHNH)]_2$.[9] However, the

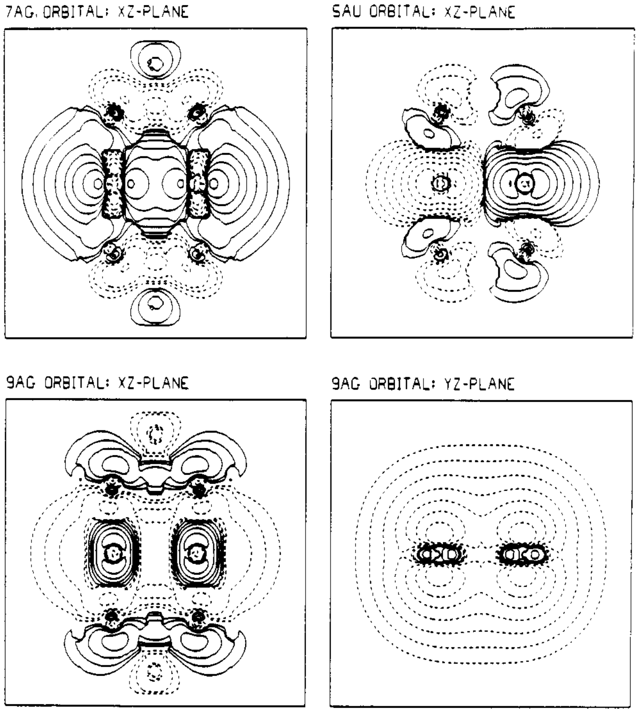

Figure 3. Contour maps of the four σ and σ^* orbitals.

Au···Au separations in many Au^I_2 compounds (Table II) are less than the sum of their van der Waals radii, 3.40 Å, suggesting that an Au···Au bonding interaction is present. Mixing of the empty $6p_z$ orbitals with the filled σ and σ^* orbitals could produce such

---

[27] Orgel, L. E. *J. Chem. Soc.* **1958**, 4186–4190.

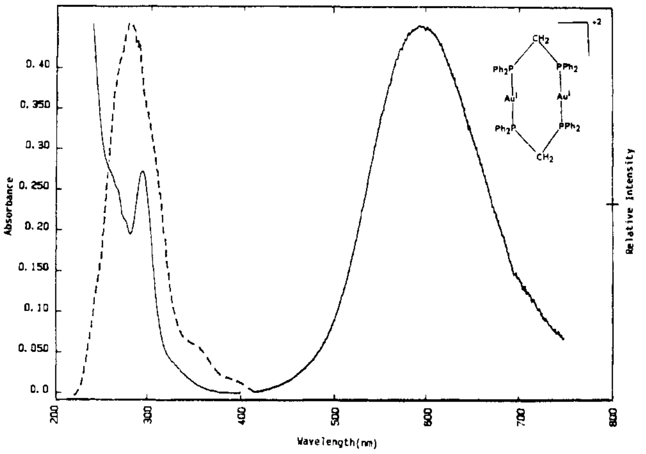

Figure 4. Excitation (- - -), absorption (—) (200–400 nm), and emission (—) (400–750 nm) spectra of $[Au(dppm)]_2(BF_4)_2$ in CH_3CN.

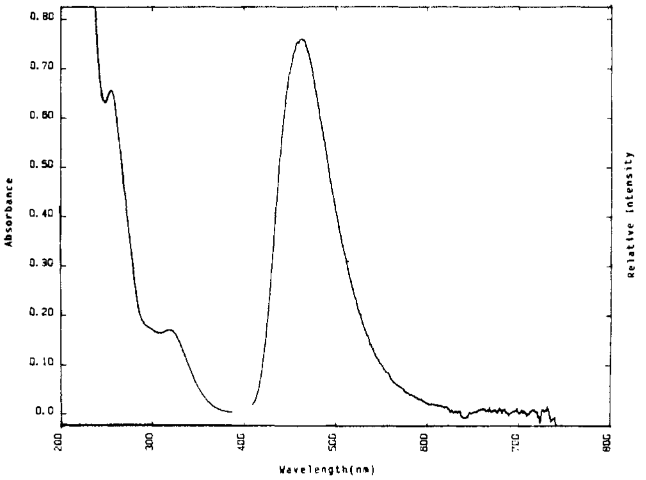

Figure 5. Absorption in CH_3CN and emission spectra of solid [Au(dppm)]$_2$Cl$_2$, 380-nm excitation.

an interaction,[8] but in $[Au_2(H_2PCH_2PH_2)_2]^{2+}$ the p_z character in the filled orbitals is negligible. The empty 6s orbital mixes with the σ and σ^* orbitals, just as it mixes with the d_{z^2} and $d_{x^2-y^2}$ orbitals in mononuclear compounds. A bonding interaction could result if the 6s orbitals mixed with the d_{z^2} orbitals so as to make the σ^* HOMO less antibonding.[8] However, in this calculation, mixing of 6s with d_{z^2} makes $7a_u$ *more* antibonding: the eigenfunctions of the 6s and d_{z^2} components on a particular gold atom have the same sign, meaning that the 6s orbitals mix with the d_{z^2} orbitals to decrease the *x* and *y* components and *increase* the antibonding axial component. Consequently, the origin of any Au···Au bonding interaction remains obscure.

The Xα–SW method works best on spherical molecules. Because this molecule is flat, the empty orbitals are poorly defined, since most of their electron density lies in the intersphere and outer-sphere regions. Therefore, the relative energies of the empty orbitals are unreliable. In fact, the order may prove to be wrong, since, if no ligand character were mixed in, the $\sigma(p_z)$ orbital $10a_u$ would lie below the $\pi(p_y)$ orbital $9b_u$.

Luminescence. The spectrum of the yellow emission of $[Au(dppm)]_2(BF_4)_2$ in CH_3CN is shown in Figure 4. The excitation spectrum resembles the absorption spectrum (Figure 4). The intense absorption from 220 to 250 nm is also found in the free ligand and is attributed to transitions within the phenyl rings. The band at 293 nm (ϵ 21 000 M^{-1} cm^{-1}) corresponds to the band at 269 nm (ϵ 24 700) in $[Au(Me_2PCH_2PMe_2)]_2^{2+}$.[4] This band is assigned to the allowed transition $^1A_u \leftarrow {}^1A_g$ ($10a_g \leftarrow 7a_u$), which is $\sigma(p_z) \leftarrow \sigma^*(s,d_{z^2})$ in nature. The emission is quenched by oxygen; in the absence of oxygen the lifetime of the excited state is 21 μs (Table II). The long lifetime and large (17 000 cm^{-1}) separation between absorption and emission suggest that the emission is phosphorescence due to the transition $^3A_u \rightarrow {}^1A_g$. The large separation also suggests that a large change in geometry, such as a shortening of the Au···Au separation, occurs in the excited state. Although the metal–metal stretching frequency may change in the excited state, no vibrational fine structure due to such a stretch was observed at 77 or 300 K in either solution, frozen glass, or solid. Large single crystals of $[Au(dppm)]_2(BF_4)_2$ were not observed to luminesce until finely powdered with a spatula.

This compound may seem to be a good candidate for doing excited-state chemistry: it has a long excited-state lifetime, 21 μs, a high excited-state energy, λ_{max} = 593 nm (48 kcal/mol), and a large emission quantum yield, 0.31 (5). However, the ground state appears to be difficult to oxidize since no gold(II) analogue, such as $[ClAu(dppm)]_2(BF_4)_2$,[28] has been reported.[13]

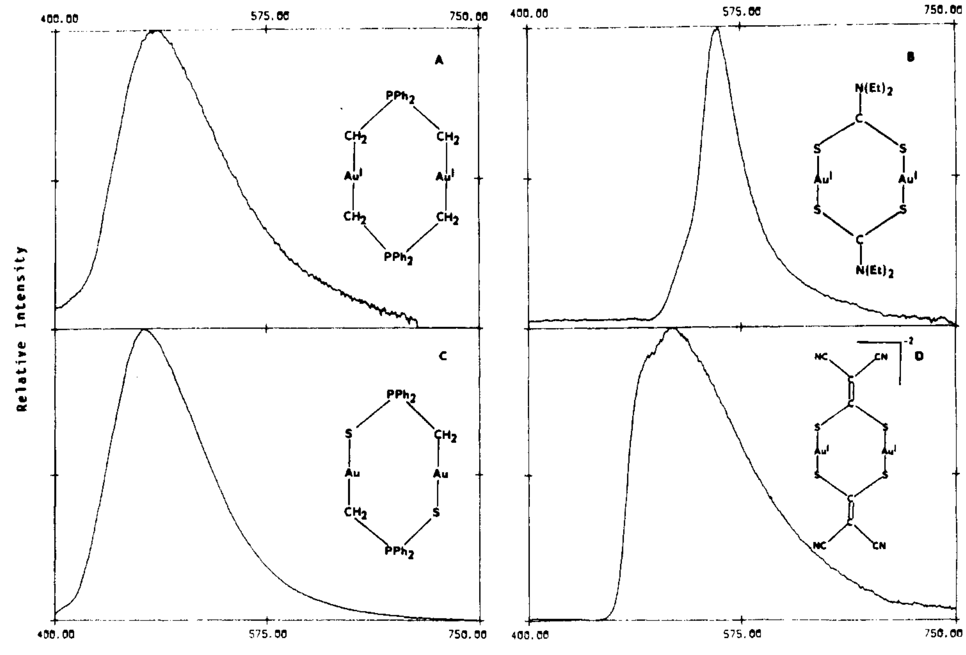

Figure 6. Emission spectra of room-temperature solids: (A) $[Au(CH_2)_2PPh_2)]_2$, 350-nm excitation; (B) $[Au(S_2CNEt_2)]_2$, 370-nm excitation; (C) $[Au(CH_2P(S)Ph_2)]_2$, 318-nm excitation; (D) $(n\text{-}Bu_4N)_2[Au(S_2C{=}C(CN)_2)]_2$, 350-nm excitation.

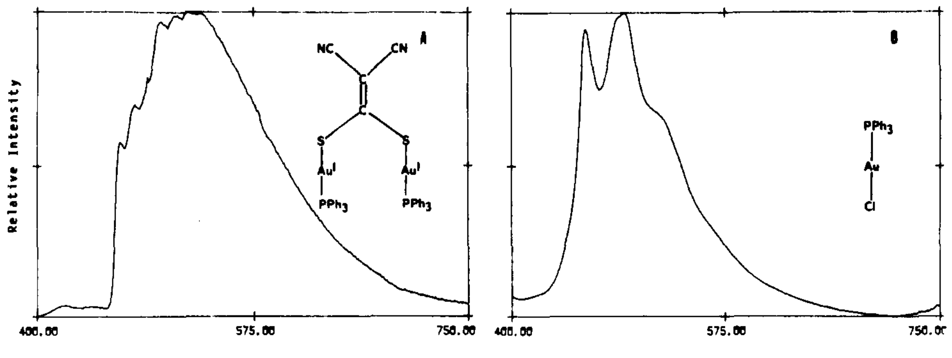

Figure 7. Emission spectra of (A) one crystal of $(Ph_3PAu)_2(S_2C{=}C(CN)_2)$ at 77 K, 350-nm excitation and (B) crystals of Ph_3PAuCl at room temperature, 330 nm-excitation.

No reaction with CH_2Cl_2 was observed after irradiation for $^1/_2$ h, although both $CHCl_3$ and CCl_4 immediately quench the emission.

The emission properties are influenced by the counterion. The BF_4^- anion does not interact with the Au atoms in the crystal. The NO_3^- salt has a weak O–Au interaction in the crystal, which is not luminescent, even when crushed. In solution this salt has the same absorption and emission spectra as the BF_4^- salt, indicating that it has dissociated. However, nitrate also quenched emission from solution. The excited-state lifetime of a concentrated solution, 15 μs, increased to ca. 22 μs on dilution; the emission spectrum did not change.

Chloride coordinates to gold in crystals of $[Au(dppm)]_2Cl_2$ to give the gold a T-shaped geometry with an Au⋯Au–Cl angle of 97°.[10] This solid has a bright blue luminescence (Figure 5 and Table II). The chloride only partially dissociates in solution: the 254-nm (ϵ 27 000 M^{-1} cm^{-1}) and 320-nm (ϵ 7000) absorption bands differ from those of the other salts (Figure 5), and the conductivity for the Cl^- salt is less ($\lambda_0 = 36\ \Omega^{-1}\ cm^{-2}\ mol^{-1}$) than that for the BPh_4^- salt[10] ($\lambda_0 = 83$). In dilute solution the chloride salt luminesces yellow, as do the other salts, but the excited-state lifetime is shorter and has two first-order components of 1.2 and 3.9 μs. Addition of excess Cl^- to the BF_4^- salt quenches emission. The blue emission of the solid was never observed from solution. Possible explanations are (1) $[Au(dppm)]_2Cl_2$ or $[Au(dppm)]_2Cl^+$ is not luminescent in solution and (2) rapid association and dissociation of Cl^- open a nonradiative path to the ground state.

The BH_3CN^- anion does not interact with the Au atoms in crystals of $[Au(dppm)]_2(BH_3CN)_2$. The solid luminesces yellow, and the solution has the same absorption spectrum as the BF_4^- and NO_3^- salts. However, the BH_3CN^- salt has a shorter solution lifetime, 3.6 μs, and decomposes on irradiation. The possible photochemistry of this salt was not further studied because solutions of $[Au(dppm)]_2^{2+}$ also react thermally with excess BH_3CN^- (see Experimental Section).

The only species reported here from which emission was observed in solution is $[Au(dppm)]_2^{2+}$. The other Au^I_2 compounds examined only phosphoresced in the solid at room temperature. The compound $[Au(CH_2)_2PPh_2]_2$ is weakly luminescent in the solid (Figure 6). No luminescence was observed from CH_2Cl_2, CH_3CN, or THF solutions. Crystals of $[Au(CH_2P(S)Ph_2)]_2$, $[n\text{-}Bu_4N]_2[Au(S_2C{=}C(CN)_2)]_2$, and $[Au(S_2CNEt)]_2$ are brightly luminescent; their emission spectra are also shown in Figure 6. the lifetime of $[Au(S_2CNEt)]_2$ could not be accurately measured because the orange solid turned brown when irradiated with the laser. The excited-state decay of several of these solids fit a competing first- and second-order rate law. The second-order term suggests that triplet–triplet annihilation occurs in the solid. These triplets may initially have been neighbors, or they may have migrated together within the solid.

Crystals of the mononuclear compound Ph_3PAuCl are also luminescent (Figure 7). The pattern of four bands in its emission spectrum is also seen in the emission spectrum of Ph_3PCuBr.[3] The compound $(Au(PPh_3))_2(S_2C{=}C(CN)_2)$ is intermediate between mononuclear and binuclear compounds, having a long Au⋯Au separation of 3.156 Å. Crystals of this compound are not luminescent at room temperature, but at 77 K they too are brightly luminescent (Figure 7).

Changing the separation between the two metals might be expected to change the energy between $\sigma^*(s,d_{z^2})$ and $\sigma(p_z)$.[29] However, emission energy does not correlate with Au⋯Au separation (Table II). This lack of correlation may be due to direct and indirect ligand effects. The HOMO has 6% ligand character, so changing the ligands will directly affect the energy of the HOMO. Indirectly, changing the ligands may change the amount of s character in other orbitals and so change the amount of s character available for mixing into the HOMO.

Phosphorescence due to this $\sigma \rightarrow \sigma^*$ transition has been observed from compounds in which the metal is four-, three-, and now two-coordinate. Every Au^I_2 compound we have examined has been found to be luminescent. Emission has been observed from dianionic, neutral, and dicationic Au^I_2 compounds with sulfur-, carbon-, and phosphorus-coordinated bridging ligands, suggesting that phosphorescence is a basic property of binuclear gold(I) compounds.

Acknowledgment. We thank Dr. Xuejun Feng for assistance with the MO calculations and for a preprint of ref 9. Lifetime measurements were obtained at the Center for Fast Kinetics Research, which is supported jointly by the Biotechnology Branch of Research Resources of the NIH (Grant RR 00886) and by The University of Texas at Austin. This work was supported by the Welch Foundation and the National Science Foundation (Grant CHE 8708625).

Note Added in Proof. The lowest energy band in the absorption spectrum of $[Au(Me_2PCH_2PMe_2)]_2^{2+}$, which is reported to luminesce in the solid state, has been assigned,[30] by using magnetic circular dichroism, to $\sigma(p_z) \leftarrow \sigma^*(d_{z^2})$.

Registry No. $[Au(H_2PCH_2PH_2)]_2^{2+}$, 120231-14-3; $[Au(dppm)]_2(BF_4)_2$, 120205-47-2; $[Au(dppm)]_2Cl_2$, 120231-15-4; $[Au(dppm)]_2(BH_3CN)_2$, 120205-41-6; $[Au(dppm)]_2(NO_3)_2$, 120231-16-5; $[Au(CH_2(S)PPh_2)]_2$, 88272-19-9; $[Au(S_2C{=}C(CN)_2)]_2(n\text{-}Bu_4N)_2$, 114131-19-0; $(Ph_3PAu)_2(S_2C{=}C(CN)_2)$, 115467-70-4; Ph_3PAuCl, 14243-64-2; $[Au(CH_2)_2PPh_2]_2$, 81457-56-9; $[Au(S_2CNEt_2)]_2$, 66712-10-5.

---

(28) We have made several unsuccessful attempts to make this compound.

(29) Mann, K. R.; Thich, J. A.; Bell, R. A.; Coyle, C. L.; Gray, H. B. *Inorg. Chem.* **1980**, *19*, 2462–2468.

(30) Jaw, H.-R.; Savas, M. M.; Rogers, R. D.; Mason, W. R. *Inorg. Chem.* **1989**, *28*, 1028–1037.